

## Article

# Response Analysis of Curved Tunnel under Near-Field Long-Period Ground Motion Considering Seismic Wave Propagation Effect

Shaofeng Liu \*, Luyan Yao, Xiaojiu Feng and Peng Wang

Department of College of Urban Construction, Changzhou University, Changzhou 213164, China

\* Correspondence: sfliu@cczu.edu.cn

**Abstract:** In this paper, long-period ground motion is used as the dynamic input to study the performance evolution of curved tunnel lining structure under seismic wave propagation excitation. This paper presents numerical studies on seismic waves, considering propagation effect, and aims to illustrate the response principle and structural failure mechanism of tunnel structures under long-period ground motion. Firstly, based on the dynamic analysis method, the dynamic balance equation of a tunnel under the seismic wave effect was analyzed. Secondly, this equation was applied to the 3D finite element software, the corresponding numerical model and boundary conditions were established, and the parameterized numerical analysis of the tunnel was carried out. Finally, according to the numerical simulation results, the seismic response principle and structural failure mechanism of a tunnel structure under long-period ground motion were discussed. The research results show that the depth and segment thickness of the tunnel significantly affect the seismic performance of the tunnel. The seismic response mechanism of a curved tunnel is complex, which shows that the relative displacements on the left and right symmetrical positions are different. The displacement inside the curve is less than the displacement outside the curve. Compared with other types of ground motion, the near-site motion considering the seismic wave propagation effect can lead to large deformation of the tunnel, which damages the lining structure greatly, and the enhancement effect is prominent for the long shield tunnel.

**Keywords:** curved tunnel; long-period ground motion; seismic wave propagation effect; seismic response analysis



**Citation:** Liu, S.; Yao, L.; Feng, X.; Wang, P. Response Analysis of Curved Tunnel under Near-Field Long-Period Ground Motion Considering Seismic Wave Propagation Effect. *Sustainability* **2023**, *15*, 60. <https://doi.org/10.3390/su15010060>

Academic Editors: Danqing Song, Zhuo Chen, Mengxin Liu and Yutian Ke

Received: 21 November 2022

Revised: 12 December 2022

Accepted: 18 December 2022

Published: 21 December 2022



**Copyright:** © 2022 by the authors. Licensee MDPI, Basel, Switzerland. This article is an open access article distributed under the terms and conditions of the Creative Commons Attribution (CC BY) license (<https://creativecommons.org/licenses/by/4.0/>).

## 1. Introduction

In the era of rapid development in China, subway tunnels are becoming more and more important in the construction of urbanization [1]. Therefore, it is an important research direction to ensure the safety and normal operation of subway tunnels. Song proposed an energy-based identification method to investigate the seismic failure mechanism [2] and obtained natural frequencies by using modal analysis and Fourier spectrum analysis [3]. Generally speaking, the damage of large-span infrastructure, such as tunnels in long-period earthquakes, is obviously more serious than ordinary earthquakes. The reason for this phenomenon is that low-frequency components in long-period seismic waves have a greater impact on long-span structures [4]. For instance: (1) the Kobe earthquake in Japan in 1995 was the first large-scale earthquake damage to modern underground tunnel structures [5–7]. (2) An earthquake with  $M = 7.3$  occurred in Nantou County, Taiwan Province in 1999. An investigation of a total of 57 tunnels revealed that 49 of them suffered damage of varying degrees. A total of 57 tunnels were investigated and 49 tunnels were found to be damaged in different degrees [8,9]. Among the 44 damaged tunnels within 25 km from the earthquake fault in Central Taiwan Province, there were 11 seriously damaged tunnels, 9 moderately damaged tunnels and 24 slightly damaged tunnels. (3) In the 2008 Wenchuan earthquake, some tunnel structures suffered earthquake damage of

different degrees (magnitude 8.0). The statistical results showed that 17.3% of them were severely damaged, 19.2% moderately damaged, 44.2% slightly damaged, and 19.3% had no obvious damage [10,11]. The post-earthquake investigation revealed that there are a lot of long-period earthquakes. Therefore, it is necessary to study the seismic performance of underground tunnel. Maleska used the DIANA program based on the Finite Element Method (FEM) to conduct a Soil–Steel Bridge analysis. Under the action of an earthquake, the influence of expanded polystyrene (EPS) geofoam block on the structure is studied [12]. In addition, Maleska used finite element software to study the type of tunnel steel shell under seismic excitation and the influence, finite element model to study the seismic performance of large-span corrugated steel plate CSP culverts [13,14]. Oskouei studied the influence of longitudinal wave propagation methods on the nonlinear strain of pipelines [15]. Abate studied the importance of soil–tunnel–building fully coupled analysis, and then discussed the influence of input frequency, tunnel depth, and building location on the seismic response of the tunnel ground structure system [16].

It is considered that long-period ground motion can be divided into two categories: near-field long-period ground motion and far-field long-period ground motion. Near-field long-period ground motion is called near-fault pulsed ground motion [17–20]. The distant field long-period ground motion is called the distant field kind harmonic ground motion [21,22]. In recent years, the influence of near fault pulse ground motion on underground structures has been widely studied by scholars. As a special kind of ground motion, near fault pulse ground motion has the characteristics of long-period and high-amplitude pulse [23]. It contains a lot of energy, which will be input into the structure in a short time, causing damage to the structure [24,25]. Anderson and Bertero [26] have shown that the increase in ground velocity caused by relatively long acceleration pulses can cause huge damage to various structures. Brun et al. [27] studied the damage potential of low-level near-field earthquakes to low-level shear walls. Near fault-like pulse ground motion causes great damage to tunnel structures. The response of surrounding rock and lining increases with the propagation of seismic waves [28]. Sun et al. [29] used nonlinear time history method to study the seismic performance of arch hydraulic tunnel, and found that the deformation of near-fault ground motion is greater than that of other types of seismic motion. Chen and Cui et al. [30,31] studied the damage of tunnels caused by ground motion. The results show that an earthquake with velocity pulse is the main factor affecting tunnel seismic damage.

The input ground motion of the tunnel dynamic response includes consistent and non-uniform conditions. At present, scholars have carried out systematic research on the deformation and structural force characteristics of the surrounding rock of the tunnel under the consistent ground motion input conditions and have obtained rich research results [32–35]. As a large flexible structure, the tunnel passing through the site soil is more complex. The spatial variation of ground motion may cause complex spatial vibration of the structure, so that it will cause more serious damage to the structure. At this time, the spatial variation of ground motion has a significant influence on the seismic response of underground structures. Chen et al. [36] used time history analysis method to study the influence of seismic ground motion on long buried immersed tunnel. The results show that SVEGM can significantly expand the seismic response of buried tunnel. Yan and Yu et al. [37,38] used the shaking table to study the response of the simulated tunnel under the non-uniform seismic load. The results show that the response of the tunnel under non-uniform seismic excitation is higher than that under uniform seismic excitation. Han et al. [39] studied the response of pipeline to non-uniform seismic excitation, and found that tunnel sliding is more likely to occur under non-uniform seismic excitation.

However, in the current research, the seismic response characteristics of curved tunnel under near-field earthquake action have not been fully understood. There is a lack of research on the effect of seismic wave propagation effect on subway tunnel. For example, S. V. Kuznetsov [40] studied the ideas for these barriers which are based on one Chadwick's result concerning non-propagation conditions for Rayleigh waves in a clamped halfspace,

and Love's theorem that describes condition of nonexistence for Love waves. In order to study the influence of seismic performance of a tunnel on the response characteristics of subway tunnel, the evolution law of performance of curved tunnel lining structure under seismic wave propagation excitation was studied with long-period ground motion as the dynamic input. Based on numerical simulation analysis, the most unfavorable section and position of curved tunnels under long-period earthquakes are found out, and the corresponding deformation law and failure mechanism of lining are pointed out. The research results further improve the theory of seismic design of tunnels, which can not only directly guide the seismic design and shock absorption measures of new tunnels, but also provide important theoretical support and data support for geological forecast, safe operation, and management of existing tunnels.

## 2. Dynamic Equation of a Tunnel under Seismic Wave Propagation Effect

The propagation speed of seismic wave is a finite value, and because the distance between the source and the ground is different, the received seismic wave must have a time lag; that is, phase difference. Therefore, the non-uniform vibration of the ground exists objectively. At present, the seismic wave propagation method is used to study the non-uniform input seismic response of tunnels. The seismic wave propagation method has the following assumptions: the ground conditions are the same, the velocity of the seismic wave along the ground is certain, the waveform at each support is the same, and only amplitude attenuation and time lag exist. The assumptions of seismic wave propagation method have some limitations, but they can reflect the characteristics of seismic wave propagation to a certain extent. The soil tunnel system is regarded as composed of tunnel structure and soil, and the seismic dynamic equation is as follows:

$$\begin{bmatrix} M_{ss} & M_{sb} \\ M_{bs} & M_{bb} \end{bmatrix} \begin{Bmatrix} \ddot{U}_{ss} \\ \ddot{U}_{bb} \end{Bmatrix} + \begin{bmatrix} C_{ss} & C_{sb} \\ C_{bs} & C_{bb} \end{bmatrix} \begin{Bmatrix} \dot{U}_{ss} \\ \dot{U}_{bb} \end{Bmatrix} + \begin{bmatrix} C_{ss} & C_{sb} \\ C_{bs} & C_{bb} \end{bmatrix} \begin{Bmatrix} U_{ss} \\ U_{bb} \end{Bmatrix} = \begin{Bmatrix} R_{ss} \\ 0 \end{Bmatrix} \quad (1)$$

where  $[M_{ss}]$ ,  $[C_{ss}]$ ,  $[K_{ss}]$  are the mass matrix, damping matrix and stiffness matrix of the tunnel;  $[M_{bb}]$ ,  $[C_{bb}]$ ,  $[K_{bb}]$  are the mass matrix, damping matrix and stiffness matrix of soil around the tunnel;  $[M_{sb}]$ ,  $[M_{bs}]$ ,  $[C_{sb}]$ ,  $[C_{bs}]$ ,  $[K_{sb}]$ ,  $[K_{bs}]$  are the coupling mass matrix, coupling damping matrix and coupling stiffness matrix between tunnel and surrounding soil;  $\ddot{U}_{ss}$ ,  $\dot{U}_{ss}$ ,  $U_{ss}$  are the acceleration, velocity and displacement of tunnel;  $\ddot{U}_{bb}$ ,  $\dot{U}_{bb}$ ,  $U_{bb}$  are the acceleration, velocity and displacement at each node of the support;  $R_{ss}$  is the external force vector acting on the tunnel; and  $R_{bb}$  is the external force vector acting on each node of soil.

Based on the relative motion method used in finite element software, the dynamic equation of the discrete model of curved tunnel under seismic wave propagation effect is derived. The total displacement in Equation (1) is decomposed into the sum of pseudo static displacement and dynamic displacement, and the dynamic response term at each node is zero, then:

$$\begin{Bmatrix} U_{ss} \\ U_{bb} \end{Bmatrix} = \begin{Bmatrix} U_{ss}^s \\ U_{bb} \end{Bmatrix} + \begin{Bmatrix} U_{ss}^d \\ 0 \end{Bmatrix} \quad (2)$$

where  $U_{ss}^s$  is the pseudo static displacement response of the structure and  $U_{ss}^d$  is the tunnel displacement response caused by the input ground motion.

In quasi-static, the dynamic term  $U_{ss}^d = 0$ , then:

$$\{U_{ss}^s\} = -[K_{ss}]^{-1}[K_{sb}]\{U_{bb}\} \quad (3)$$

Let  $[R] = -[K_{ss}]^{-1}[K_{sb}]$ , which is called the influence matrix, and represent the relationship between the bottom movement items of soil and the quasi-static items of structure. Therefore, by substituting Equations (2) and (3) into Equation (1), the tunnel dynamic balance equation based on relative motion method can be obtained:

$$[M_{ss}]\{\ddot{U}_{ss}^d\} + [C_{ss}]\{\dot{U}_{ss}^d\} + [K_{ss}]\{U_{ss}^d\} = -[M_{ss}][R]\{\ddot{U}_{bb}\} \quad (4)$$

In this paper, the longitudinal horizontal seismic input is considered in the curved tunnel, and the seismic wave propagation effect of ground motion is simulated by phase difference, which is to say,  $U$  with different time delays  $\ddot{U}_{bb}$  input ground motion. Based on the finite element software, the relative motion can be used to solve the tunnel seismic response. Considering the influence of seismic wave propagation effect on the structure, the acceleration on the right side of Equation (4) is determined by the ground motion acceleration vector at each support according to the same seismic wave acceleration record with a certain time difference.

### 3. Numerical Models

A series of numerical models are constructed by using three-dimensional finite element software to simulate the propagation of seismic waves in infinite or semi-infinite media. The model size is set to 400 m (length)  $\times$  200 m (width)  $\times$  70 m (height), and the tunnel radius is set to 3.2 m. The elastic–plastic constitutive model without dilatancy Mohr–Coulomb shear failure criterion is used to study the influence of soil nonlinearity [41]. The tunnel lining is made of C50 concrete with a thickness of 0.4 m and a reinforcement ratio of 0.6%. The plastic damage model is used to simulate the concrete [42]. The properties of soil and tunnel lining are shown in Table 1. The material damping of soil is assumed to be 5% [43]. In the existing boundary conditions, the non-reflecting boundaries are applied along the lateral boundaries to properly absorb the outward waves. The upper part is the free surface, the surroundings are set as the free field boundary, and the bottom of the model is the rigid base condition. In addition, in order to simulate the entrance and exit of the tunnel more realistically, a hinged bracket was set at the entrance and exit to simulate the reinforced concrete front wall [44]. The schematic diagram of the 3D model and the boundary conditions are shown in Figure 1, where  $D$  is the buried depth and  $B$  is the tunnel diameter. It is worth mentioning that this work is first academic research. Nevertheless, the soil parameter set used for the research is taken from the literature and corresponds to the real soil parameter value [45,46].

**Table 1.** Lining and soil properties.

Material	Unit Weight (kN /m <sup>3</sup> )	Elastic Modulus (MPa)	Poisson's Ratio	Cohesion (MPa)	Dilation Angle (°)
Silty clay	21	16	0.22	1.8	50
Very silty clay	20	6	0.28	1.2	40
Clay	20	3	0.32	0.8	28
Silty clay silty sand	21	13	0.30	1.9	43
Tunnel lining	25	32,500	0.3	—	—

In the seismic response analysis of curved tunnel structure, the following basic assumptions are considered:

- (1) The pipe segments bolted in the actual project are assumed to be homogeneous rings;
- (2) The soil and tunnel structure materials are assumed to be homogeneous, isotropic.

The factors affecting the seismic response of the tunnel are: (a) buried depth; (b) tunnel radius; (c) lining thickness; and (d) earthquake. In order to understand the characteristics of curved tunnels under seismic loads, this paper uses the three-dimensional finite element software, using nonlinear time history analysis, to study the effects of the above-mentioned parameters of near-field long-period ground motions on curved tunnels. The EI Centro (EI record) data from the 1940 California earthquake and the near-field seismic wave (TCU003 record) data with obvious pulse effect from the 1999 Chi Chi earthquake in Taiwan are used as dynamic input motions. The ground motion input is shown in Figure 2, and the

direction of seismic wave application is consistent with the direction of the tunnel. In order to compare the influence of near-field long-period seismic wave and ordinary seismic wave on curved tunnel under the same seismic intensity, the peak values of the two seismic waves are adjusted to be the same. In order to make the results comparable, it should be scaled down or enlarged to  $1 \text{ m/s}^2$ . Table 2 summarizes the parameter combinations in different cases. Figure 3a represents the acceleration time histories of the ground motions of the EI and TCU003 records, while Figure 3b represent the corresponding Fourier amplitude spectra of them. It is found that the EI record band is mainly distributed between 1–5 Hz, and the frequency band of TCU003 record is mainly distributed between 0–2 Hz. Compared with ordinary seismic wave EI, the low-frequency components of near-field long-period seismic waves are more abundant, and the predominant components of Fourier spectrum are more obvious.

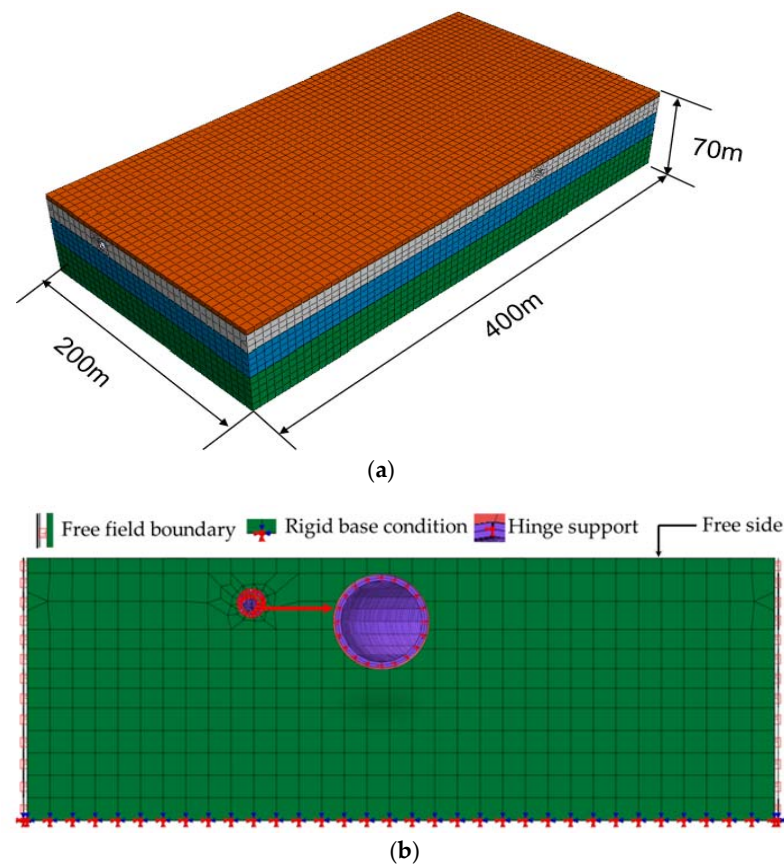


Figure 1. (a) Tunnel model condition; (b) boundary condition.

Table 2. Calculation cases.

Parameters	Lining Thickness	Depth/m	Turning Radius/m	Seismic Wave
1	0.3	12	800	EI
2	0.4	12	800	EI
3	0.5	12	800	EI
4	0.4	12	200	EI
5	0.4	12	400	EI
6	0.4	12	800	EI
7	0.4	12	800	EI
8	0.4	12	200	TCU003
9	0.4	12	400	TCU003
10	0.4	12	800	TCU003

Table 2. Cont.

Parameters	Lining Thickness	Depth/m	Turning Radius/m	Seismic Wave
11	0.4	8	200	EI (Seismic wave propagation)
12	0.4	16	400	EI (Seismic wave propagation)
13	0.4	8	800	EI (Seismic wave propagation)
14	0.4	16	200	TCU003 (Seismic wave propagation)
15	0.4	12	400	TCU003 (Seismic wave propagation)
16	0.4	12	800	TCU003 (Seismic wave propagation)

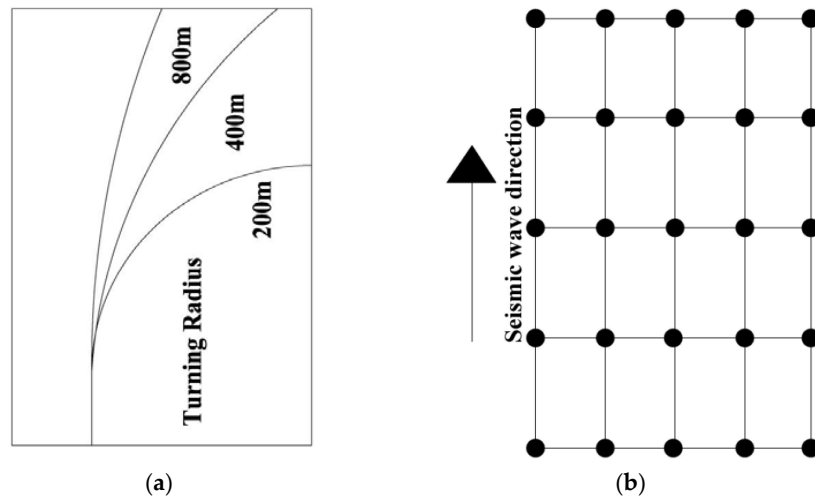


Figure 2. (a) Schematic diagram of tunnel; (b) schematic diagram of multi-point seismic wave input.

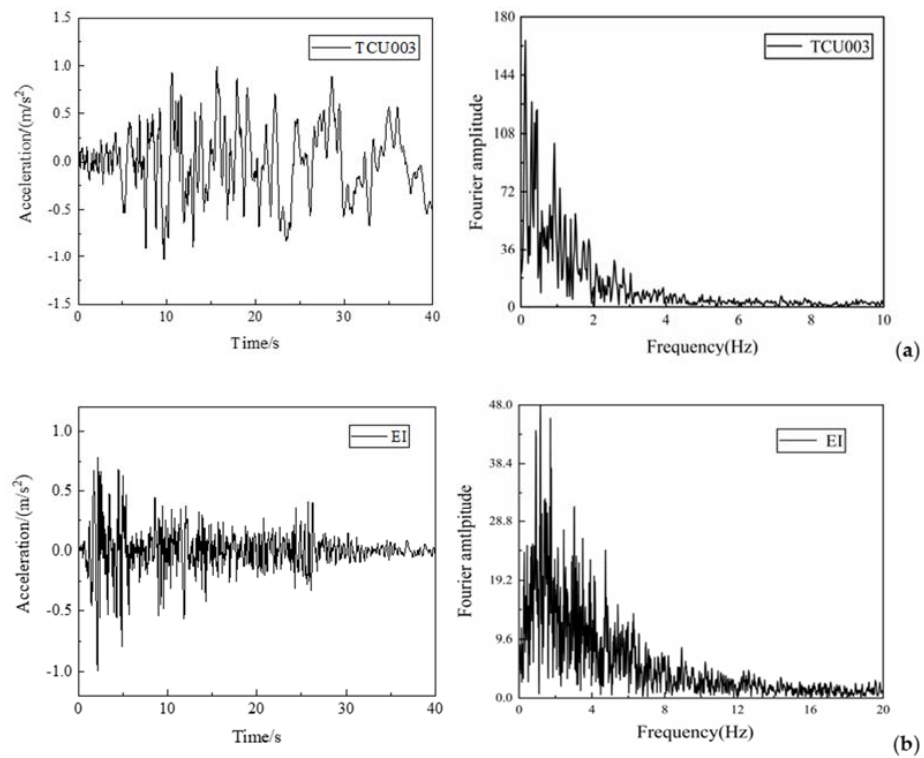
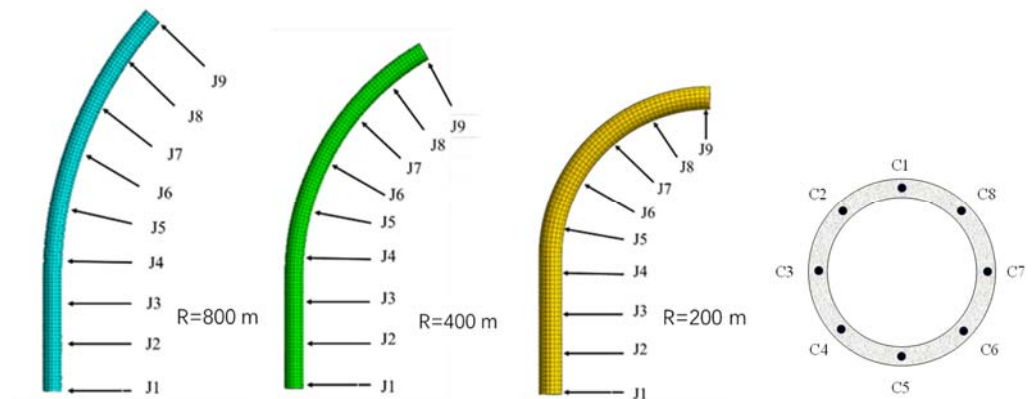


Figure 3. Acceleration time histories of input ground motions and Fourier amplitude spectra of the input motions. (a) EI record and (b) TCU003 record.

## 4. Results and Discussion

In order to reveal the mechanism of interaction between tunnel and soil, the dynamic response of tunnel to near-field long-period ground motion is analyzed by detecting the displacement and acceleration of different positions under different conditions. The corresponding monitoring points are shown in Figure 4, where  $R$  is the turning radius.



**Figure 4.** Layout of tunnel measuring points.

### 4.1. Study on Tunnel Parameterization

#### 4.1.1. Influence of Lining Thickness and Tunnel Depth

The vault displacement of each monitoring point of the tunnel under different buried depth and lining thickness is shown in Figure 5. According to Figure 5a, when  $D = 12$  m,  $R = 800$  m, with the increase in lining thickness, the peak displacement of measuring points of lining structure decreases. However, the trend of reduction gradually decreases, that is, the effect of concrete thickness changes on the displacement of lining structure gradually decreases. The results show that the appropriate increase in lining thickness is beneficial to reduce the displacement response of curved tunnel under seismic action. With other conditions unchanged, it can be seen from Figure 5b that the peak value of relative displacement is different with the buried depth changes. With the increase in tunnel depth, the amplitude of vault displacement is gradually reduced. The closer the tunnel is to the surface free field, the smaller the constraint of soil and the larger the relative displacement. The data analysis shows that the buried depth of the tunnel has a significant impact on the tunnel structure displacement under earthquake. On the whole, they are in inverse proportion.

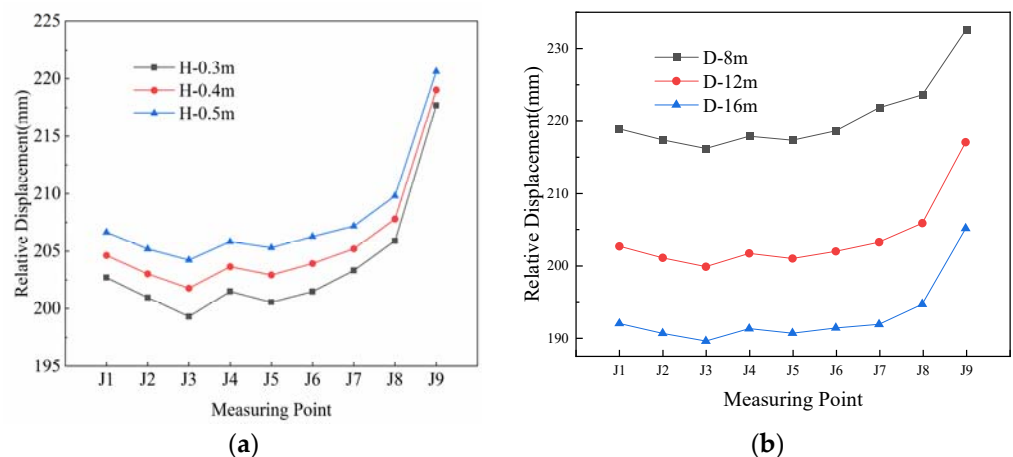


**Figure 5.** Tunnel vault displacement curve: (a) different lining thickness and (b) different buried depth.

Keeping the other parameters constant, the dynamic response of the tunnel is calculated when the lining thickness is 0.4 m and the buried depth is 12 m. The displacement of cross section of tunnel is shown in Figure 6, and C1–C8 is the section measuring point of curved tunnel structure. It can be seen from Figure 6 that at the bottom of the tunnel the displacement is the smallest, and the left and right sides gradually increase upwards. At the top of the tunnel, the displacement is the largest. The maximum displacement occurs at the tunnel vault. With the downward displacement of the measuring points, the displacement becomes smaller and smaller. The displacement reaches the minimum at the bottom of the tunnel. This is because the closer the tunnel is to the surface, the more obvious the displacement magnification effect is. The top of the tunnel is closer to the ground surface, and its displacement increases accordingly. It can be seen that the response of the model under different conditions of the structure shows certain regularity when comparing the results of the tunnel at each measuring point. For the tunnel structure with the same cross-section, the maximum value of dynamic response generally occurs at the tunnel vault, and the minimum value occurs at the bottom of the tunnel. To a certain extent, it reveals that the tunnel vault is the weak link of earthquake resistance.

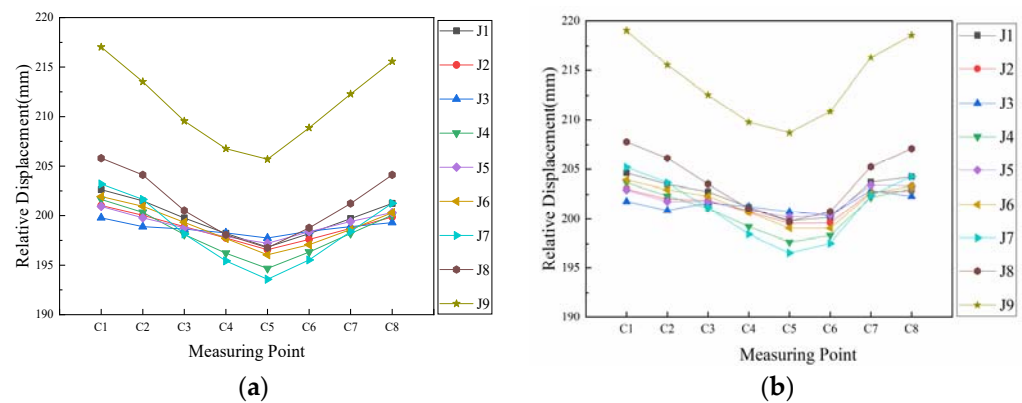


**Figure 6.** Cross section displacement peak curve (a) lining thickness  $H = 0.4$  m and (b) buried depth  $D = 12$  m.

#### 4.1.2. Influence of Turning Radius

Keeping the other parameters constant, the dynamic response of the tunnel is calculated when the turning radius is 200 m, 400 m, and 800 m, respectively. Figure 7a shows peak displacement curve of longitudinal measuring points in a tunnel extension. Figure 7b–d shows the relative displacement curves of the left and right symmetrical positions under different turning radius.

Under EI seismic load, the peak value of relative displacement is different with different turning radius. With the increase in turning radius of tunnel curve, the displacement amplitude of vault decreases gradually. However, with the change of measuring points, the relative displacement also increases gradually. It reaches the maximum at the outlet. It shows that the tunnel entrance is the weak link of earthquake resistance. The smaller the turning radius is, the greater the displacement of the tunnel will be.

As shown in Figure 7b–d, the relative displacements of the tunnel at the left and right symmetrical positions of the cross section of the straight section are basically equal. The cross section is still flat. However, the relative displacements of the left and right symmetrical positions are not equal in curved tunnels, and the cross section of the tunnel lining is twisted into a curved surface. The displacement inside the curve is smaller than that of outside the curve, and the relative displacement increases gradually with the backward movement of the measuring point. When the turning radius is 200 m, the difference reaches about 5 mm at the opening; this is the maximum of these models.

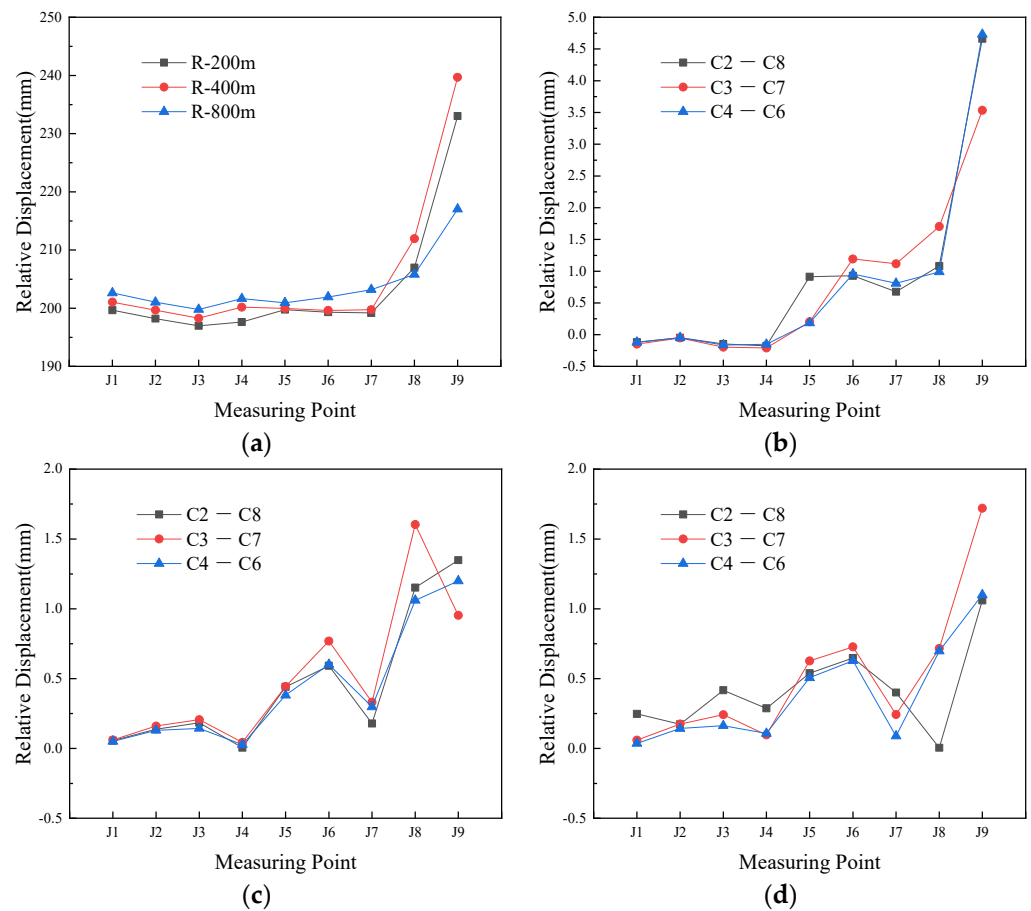


**Figure 7.** Peak displacement of vault and relative displacement of tunnel: (a) peak displacement of tunnel along different radius; (b) radius 200 m; (c) radius 400 m; and (d) radius 800 m.

#### 4.2. The Effect of Seismic Wave Propagation on a Tunnel

In the seismic analysis of underground structures, it is generally assumed that the bedrock has rigid body motion under the action of earthquake. Every point on the bedrock receives the same ground motion at the same time and ignores the spatial variation of ground motion. However, in the actual project, the movement of each point on the bedrock is not synchronous because the wave propagation needs a certain time. Due to the large span of tunnel structure, the time required for the transmission of ground motion to different parts of the structure is different. The influence of seismic wave propagation effect on structural deformation should be considered, and the influence of seismic wave propagation effect on tunnels should be simulated by non-uniform excitation.

The cross section of tunnel will be distorted under the action of earthquake, and the cross section is no longer a plane. In order to analyze the response difference under different seismic waves, it can be characterized by the displacement of each detection point of the lining relative to a certain point of the lining. The deformation displacement of the tunnel is defined as:

$$\Delta = \Delta_{C1} - \Delta_{C5} \quad (5)$$

where  $\Delta_{C1}$  is the displacement of tunnel vault and  $\Delta_{C5}$  is the displacement of tunnel bottom.

It can be seen from Figure 8 that under long-term excitation, the response of the structure with different turning radius models shows a certain degree of regularity. Meanwhile, under the same conditions but different turning radius shows some differences from the deformation of structures. Under the excitation of a long-period wave, the smaller the radius is, the larger the dynamic response and the increased relative displacement is. Compared with EI seismic excitation, the model of TCU003 has larger displacement and

deformation. When the radius is 200 m, the maximum relative displacement in TCU003 model is 27.3 mm.

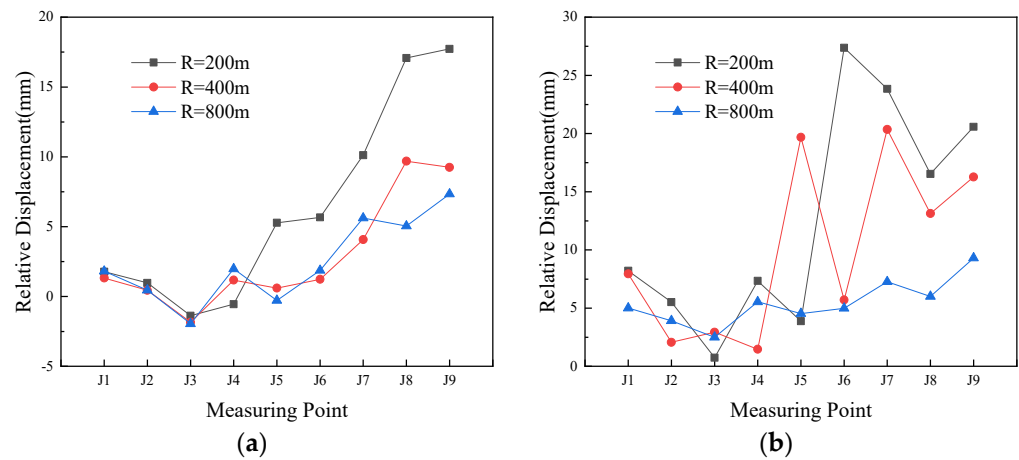


**Figure 8.** Tunnel deformation: (a) EI record and (b) TCU003 record.

Considering the seismic wave propagation effect, the variation of lining horizontal displacement along the axial direction under the action of short-period earthquakes and long-period earthquakes is shown in Figure 9, respectively. The displacement and deformation of the tunnel from the first measuring point to the third measuring point is decreasing. After the third measuring point, the trend of displacement and deformation is increasing. Compared with the ordinary seismic wave, the long-period seismic wave magnifies the deformation trend, and the deformation displacement reaches the maximum value at the position of tunnel exit. The results show that the horizontal displacement of lining has a large mutation under the action of a long-period earthquake.

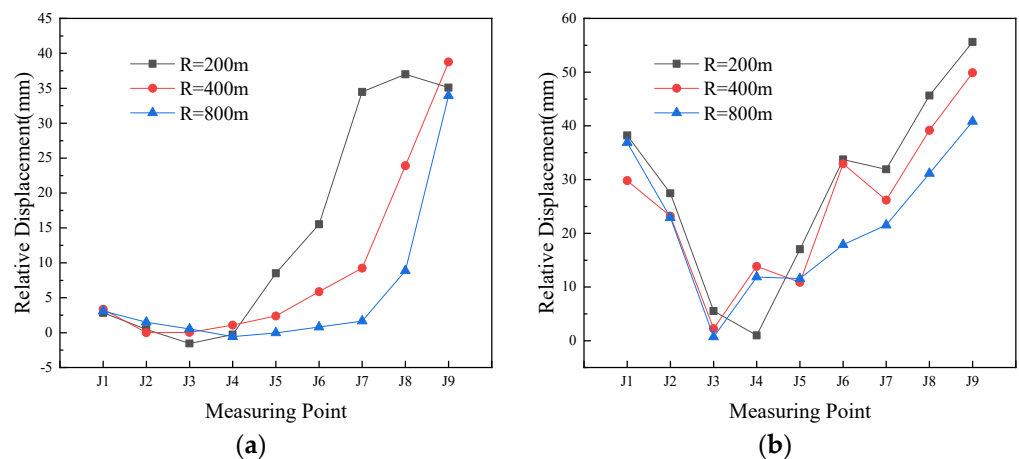


**Figure 9.** Tunnel deformation considering seismic wave propagation effect: (a) EI record and (b) TCU003 record.

From Figures 8 and 9, it can be concluded that the relative deformation of tunnel structure considering seismic wave propagation effect is greater than that of uniform excitation. In addition, it can also be seen that the entrance of the curved tunnel, the intersection of the straight line and the curve, and the maximum arc of the curve have greater displacement and deformation. Comparing the response of different seismic waves, the non-uniform effect of the structure is significant under the near-field long-term ground motion, and the relative deformation of the tunnel structure is greater. The main reason is that the internal force distribution of a tunnel structure is very complex due to the non-uniform effect of seismic waves, and the deformation direction in different parts has

certain uncertainty, as shown in the opposite deformation trend in the figure above. These conditions will have adverse effects on a tunnel structure, such as deformation, cracking and spalling of lining. In addition, the long shield tunnel is also more vulnerable to damage under the near-field long-period earthquake. Therefore, the spatial variation of ground motion and the influence of long-period earthquakes on the tunnel cannot be ignored for long and curved tunnels.

When seismic wave propagation effects are not considered, the acceleration time history and Fourier spectrograms of different seismic waves at different tunnel locations are shown in Figure 10. It can be seen from Figure 10 that the two acceleration time history curves show good consistency at different positions of the tunnel. The acceleration time history under long-period earthquake is far greater than that of control group. In addition, it can be seen from the spectrum diagram that the two seismic waves have multiple peaks in the range of 0–5 Hz. Among them, EI record has several obvious main frequencies, which are between 1–2 Hz, and the main peak value is significantly greater than other peaks. TCU003 has one peak, but its main frequency is between 0–0.5 Hz. Compared with the long-period seismic excitation, the spectrum amplitude of the short-period seismic wave is smaller, and the phenomenon of multi peak appears. The frequency band distribution is wider, and the spectrum composition is more abundant.

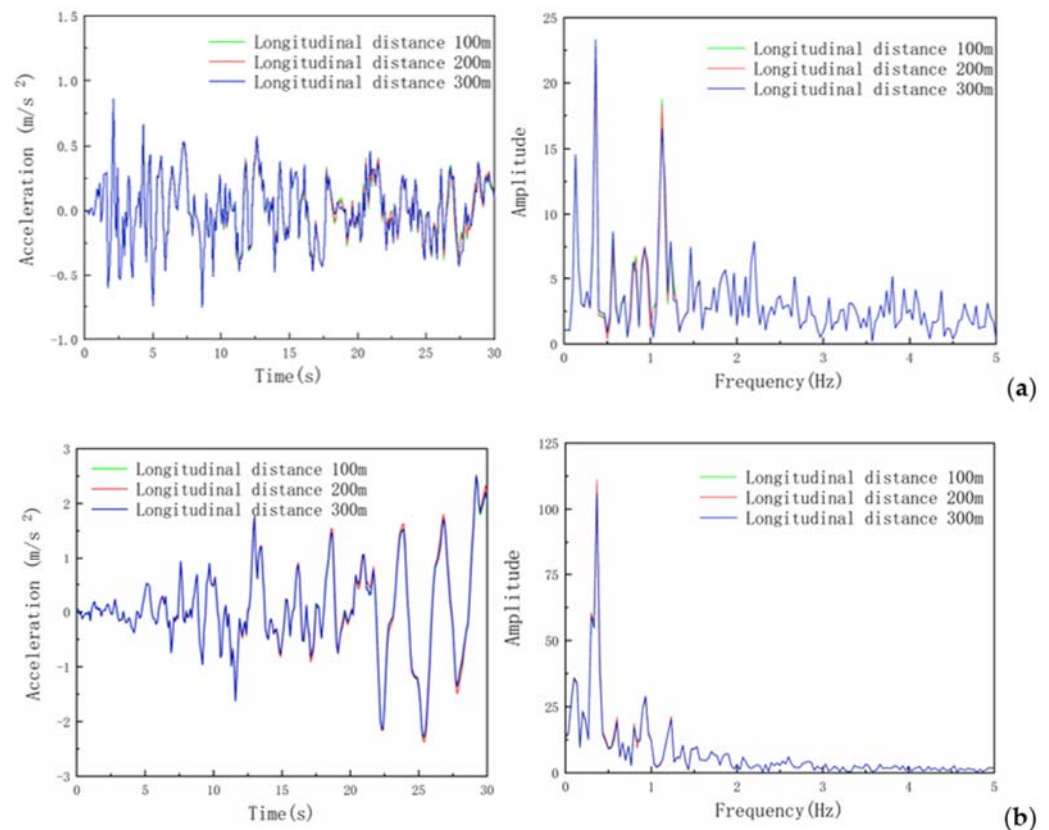


**Figure 10.** Acceleration responses of the liner top at 80 m under different waves: (a) EI record and (b) TCU003 record.

Figure 11 is the acceleration time history curve and Fourier spectrum when the turning radius is 800 m with and without seismic wave propagation. It can be seen from Figure 11 that, compared with uniform excitation, the acceleration delay phenomenon is more obvious with the increase in time, and the acceleration peak value of the tunnel shows a decreasing trend. In addition, it can be seen from the spectrum diagram that the peak value of spectrum is reduced, and the spectrum amplitude is small. The frequency band distribution is wider, and the spectrum composition is more abundant.

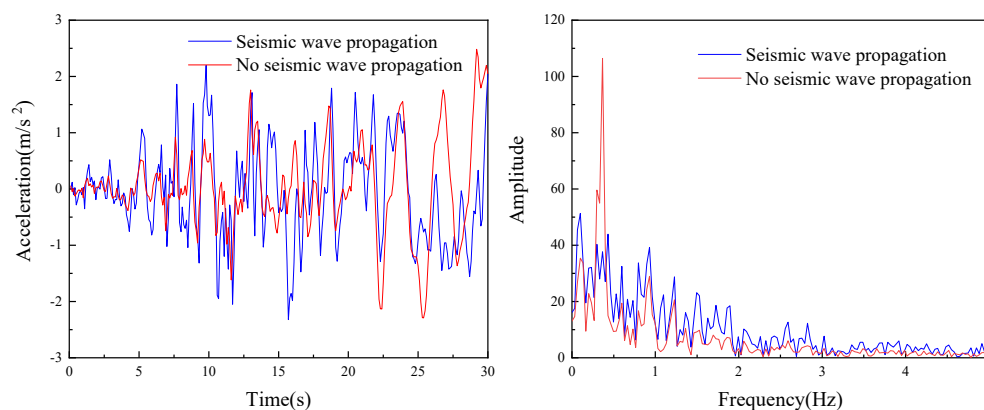


Figure 11. Acceleration responses of liner top at 800 m under different waves.

## 5. Conclusions

Based on the dynamic analysis method, the dynamic balance equation of the tunnel under the seismic wave effect is deduced. Secondly, this equation is applied to the 3D finite element software, and this paper studies the seismic performance of the tunnel under near-field long-period earthquakes. The longitudinal seismic response of long shield tunnel structure under near-field long-period ground motion is discussed. The following conclusions are obtained:

(1) In the study of tunnel parameterization, as the lining thickness and buried depth increase, the peak displacement of the tunnel structure decreases. In addition, increasing the turning radius of the tunnel can also reduce the tunnel displacement. Therefore, choosing the appropriate buried depth, lining thickness and turning radius can improve the seismic performance of the tunnel. In actual projects, in order to reduce the impact of earthquakes, reasonable burial depth, construction technology and design optimization schemes should be considered.

(2) Under seismic excitation, the maximum displacement of the tunnel occurs at the top of the tunnel section, and the shallower the buried depth of the tunnel, the greater the displacement of the top of the tunnel. In addition, compared to a straight tunnel, the displacement on the left and right sides of a curved tunnel is not equal, and the tunnel deforms more.

(3) Under the action of long-period earthquakes in the near field, the entrance of the curved tunnel, the intersection of the straight line and the curve, and the maximum arc of the curve, have large displacements and deformations. These areas are the weak links in the tunnel's earthquake resistance, and effective reinforcement measures are necessary. The research results have certain reference significance for the seismic reinforcement design of curved subways.

(4) Generally speaking, when studying the seismic performance of tunnels, the effects of near-field long-period ground motion and seismic wave propagation are generally not considered. However, this study found that for long tunnels, the effects of near-field long-period ground motion and seismic wave propagation cannot be ignored. The deformation of the tunnel caused by the long-period earthquake is more obvious, and the sudden change is larger. In addition, when the seismic wave propagation effect is considered, the seismic response is more severe than the uniform seismic excitation, and the seismic acceleration presents a certain time lag.

This paper only analyzes the dynamic response of the structure and conducts damage analysis to the structure. When conducting regional seismic damage simulation and seismic analysis of long and large underground structures, the spatial effects of ground motions should be properly considered, and more reasonable ground motion input methods should be adopted. The next step is to establish the limit state function of the tunnel through the

artificial neural network method and solve the reliability and failure probability of the tunnel, so as to quantitatively analyze the damage degree of the tunnel under earthquake.

**Author Contributions:** Methodology, S.L. and X.F.; data curation, software, S.L. and L.Y.; validation, P.W.; writing—review and editing, L.Y.; funding acquisition, S.L. All authors have read and agreed to the published version of the manuscript.

**Funding:** This research was funded by the Natural Science Foundation of the Jiangsu Higher Education Institutions of China (grant number 18KJB560001).

**Institutional Review Board Statement:** Not applicable.

**Informed Consent Statement:** Not applicable.

**Data Availability Statement:** The data used to support the findings of this study are available from the corresponding author upon request.

**Conflicts of Interest:** The authors declare no conflict of interest.

## References

1. Pitilakis, K.; Alexoudi, M.; Argyroudis, S.; Monge, O.; Martin, C. Earthquake risk assessment of lifelines. *Bull. Earthq. Eng.* **2006**, *4*, 365–390. [[CrossRef](#)]
2. Song, D.; Liu, X.; Huang, J.; Zhang, J. Energy-based analysis of seismic failure mechanism of a rock slope with discontinuities using Hilbert-Huang transform and marginal spectrum in the time-frequency domain. *Landslides* **2021**, *18*, 105–123. [[CrossRef](#)]
3. Song, D.; Liu, X.; Huang, J.; Wang, E.; Zhang, J. Characteristics of wave propagation through rock mass slopes with weak structural planes and their impacts on the seismic response characteristics of slopes: A case study in the middle reaches of Jinsha River. *Bull. Eng. Geol. Environ.* **2020**, *80*, 1317–1334. [[CrossRef](#)]
4. Dai, M.; Li, Y.; Dong, Y. Incorporation of envelope delays and amplifications into simulation of far-field long-period ground motions. *Soil Dyn. Earthq. Eng.* **2020**, *136*, 106192. [[CrossRef](#)]
5. Patil, M.; Choudhury, D.; Ranjith, P.G.; Zhao, J. Behavior of shallow tunnel in soft soil under seismic conditions. *Tunn. Undergr. Space Technol.* **2018**, *82*, 30–38. [[CrossRef](#)]
6. Ma, C.; Lu, D.; Du, X.; Qi, C. Effect of buried depth on seismic response of rectangular underground structures considering the influence of ground loss. *Soil Dyn. Earthq. Eng.* **2018**, *106*, 278–297. [[CrossRef](#)]
7. Asakura, T.; Shiba, Y.; Matsuoka, S.; Oya, T.; Yashiro, K. Damage to mountain tunnels by earthquake and its mechanism. *Doboku Gakkai Ronbunshu.* **2000**, *659*, 27–38. (In Japanese) [[CrossRef](#)]
8. Hashash, Y.M.A.; Hook, J.J.; Schmidt, B.; I-Chiang Yao, J. Seismic design and analysis of underground structures. *Tunn. Undergr. Space Technol.* **2001**, *16*, 247–293. [[CrossRef](#)]
9. Wang, W.L.; Wang, T.T.; Su, J.J.; Lin, C.H.; Seng, C.R.; Huang, T.H. Assessment of damage in mountain tunnels due to the Taiwan Chi-Chi Earthquake. *Tunn. Undergr. Space Technol.* **2001**, *16*, 133–150. [[CrossRef](#)]
10. Wang, Z.; Gao, B.; Jiang, Y.; Yuan, S. Investigation and assessment on mountain tunnels and geotechnical damage after the Wenchuan earthquake. *Sci. China Ser. E Technol. Sci.* **2009**, *52*, 546–558. [[CrossRef](#)]
11. Cui, G.; Wang, M.; Lin, G. Statistical analysis of Earthquake damage types of typical highway tunnel lining structure in Wenchuan seismic disastrous area. *Chin. J. Geol. Hazard Control.* **2011**, *22*, 122–127. [[CrossRef](#)]
12. Maleska, T.; Nowacka, J.; Beben, D. Application of EPS Geofoam to a Soil–Steel Bridge to Reduce Seismic Excitations. *Geosciences* **2019**, *9*, 448. [[CrossRef](#)]
13. Maleska, T.; Beben, D.; Nowacka, J. Seismic vulnerability of a soil-steel composite tunnel—Norway Tolpinrud Railway Tunnel Case Study. *Tunn. Undergr. Space Technol.* **2021**, *110*, 103808. [[CrossRef](#)]
14. Mahgoub, A.; Naggar, H.E. Seismic Design of Metal Arch Culverts: Design Codes Vs. Full Dynamic Analysis. *J. Earthq. Eng.* **2019**, *25*, 2231–2268. [[CrossRef](#)]
15. Oskouei, A.G.; Oskouei, A.V. The Effect of P-Wave Propagation on the Seismic Behavior of Steel Pipelines. *Period. Polytech.-Civ.* **2017**, *61*, 889–903. [[CrossRef](#)]
16. Abate, G.; Massimino, M.R. Parametric analysis of the seismic response of coupled tunnel–soil–aboveground building systems by numerical modelling. *Bull. Earthq. Eng.* **2017**, *15*, 443–467. [[CrossRef](#)]
17. Liao, W.; Loh, C.-H.; Wan, S. Earthquake responses of RC moment frames subjected to near-fault ground motions. *Struct. Des. Tall Spec. Build.* **2001**, *10*, 219–229. [[CrossRef](#)]
18. Shahi, S.K.; Baker, J.W. An Empirically Calibrated Framework for Including the Effects of Near-Fault Directivity in Probabilistic Seismic Hazard Analysis. *Bull. Seismol. Soc. Am.* **2011**, *101*, 742–755. [[CrossRef](#)]
19. Kalkan, E.; Kunnath, S.K. Effects of Fling Step and Forward Directivity on Seismic Response of Buildings. *Earthq. Spectra* **2006**, *22*, 367–390. [[CrossRef](#)]
20. Bray, J.D.; Rodriguez-Marek, A. Characterization of forward-directivity ground motions in the near-fault region. *Soil Dyn. Earthq. Eng.* **2004**, *24*, 815–828. [[CrossRef](#)]

21. Ariga, T.; Kanno, Y.; Takewaki, I. Resonant behaviour of base-isolated high-rise buildings under long-period ground motions. *Struct. Des. Tall Spec. Build.* **2006**, *15*, 325–338. [[CrossRef](#)]
22. Mai, P.M.; Imperatori, W.; Olsen, K.B. Hybrid Broadband Ground-Motion Simulations: Combining Long-Period Deterministic Synthetics with High-Frequency Multiple S-to-S Backscattering. *Bull. Seismol. Soc. Am.* **2010**, *100*, 2124–2142. [[CrossRef](#)]
23. Chang, Z.; Sun, X.; Zhai, C.; Zhao, J.X.; Xie, L. An improved energy-based approach for selecting pulse-like ground motions. *Earthq. Eng. Struct. Dyn.* **2016**, *45*, 2405–2411. [[CrossRef](#)]
24. Fathi, M.A.; Makhdoumi, M. Parvizi. Effect of supplemental damping on seismic response of base isolated frames under near & far field accelerations, *Ksce. J. Civ. Eng.* **2015**, *19*, 1359–1365. [[CrossRef](#)]
25. Yang, D.; Pan, J.; Li, G. Non-structure-specific intensity measure parameters and characteristic period of near-fault ground motions. *Earthq. Eng. Struct. D* **2009**, *38*, 1257–1280. [[CrossRef](#)]
26. Anderson, J.; Bertero, V. Uncertainties in establishing design earthquakes. *J. Struct. Eng.* **1987**, *113*, 1709–1724. [[CrossRef](#)]
27. Brun, M.; Reynouard, J.M.; Jezequel, L.; Ile, N. Damaging potential of low-magnitude near-field earthquakes on low-rise shear walls. *Soil Dyn. Earthq. Eng.* **2004**, *24*, 587–603. [[CrossRef](#)]
28. Zhao, X.; Shuping, J.; Yi, Y. Study on Shaking Table Model Test Scheme of Tunnel Subjected to Near-Fault Pulse-Like Ground Motions. *Mod. Appl. Sci.* **2014**, *8*, 126–139. [[CrossRef](#)]
29. Sun, B.; Zhang, S.; Deng, M.; Wang, C. Inelastic dynamic response and fragility analysis of arched hydraulic tunnels under as-recorded far-fault and near-fault ground motions. *Soil Dyn. Earthq. Eng.* **2020**, *132*, 106070. [[CrossRef](#)]
30. Chen, Z.; Wei, J. Correlation between ground motion parameters and lining damage indices for mountain tunnels. *Nat. Hazards* **2013**, *65*, 1683–1702. [[CrossRef](#)]
31. Cui, Z.; Sheng, Q.; Leng, X. Effects of a controlling geological discontinuity on the seismic stability of an underground cavern subjected to near-fault ground motions. *Bull. Eng. Geol. Environ.* **2018**, *77*, 265–282. [[CrossRef](#)]
32. Chen, Z.; Liang, S.; Shen, H. Dynamic centrifuge tests on effects of isolation layer and cross-section dimensions on shield tunnels. *Soil Dyn. Earthq. Eng.* **2018**, *109*, 173–187. [[CrossRef](#)]
33. Jza, B.; Yong, Y.; Zhen, B.D. Shaking table tests on shaft-tunnel junction under longitudinal excitations. *Soil Dyn. Earthq. Eng.* **2020**, *132*, 106055. [[CrossRef](#)]
34. Chen, Z.Y.; Shen, H. Dynamic centrifuge tests on isolation mechanism of tunnels subjected to seismic shaking. *Tunn. Undergr. Space Technol.* **2014**, *42*, 67–77. [[CrossRef](#)]
35. Zhang, J.; Yuan, Y.; Yu, H. Shaking table tests on discrepant responses of shaft-tunnel junction in soft soil under transverse excitations. *Soil Dyn. Earthq. Eng.* **2019**, *120*, 345–359. [[CrossRef](#)]
36. Chen, Z.Y.; Liang, S.B.; He, C. Influence of Incoherence and Wave Passage Effects on Seismic Performances of Long Immersed Tunnel. *Int. J. Comput. Methods* **2017**, *16*, 1840012. [[CrossRef](#)]
37. Yan, X.; Yuan, J.; Yu, H. Multi-point shaking table test design for long tunnels under non-uniform seismic loading. *Tunn. Undergr. Space Technol.* **2016**, *59*, 114–126. [[CrossRef](#)]
38. Yu, H.; Yuan, Y.; Xu, G.; Su, Q.; Yan, X.; Li, C. Multi-point shaking table test for long tunnels subjected to non-uniform seismic loadings-part II: Application to the HZM immersed tunnel. *Soil Dyn. Earthq. Eng.* **2018**, *108*, 187–195. [[CrossRef](#)]
39. Han, J.; El Naggar, M.H.; Zhao, M.; Zhong, Z.; Hou, B.; DU, X. Longitudinal response of buried pipeline under non-uniform seismic excitation from multi-point shaking table tests. *Soil Dyn. Earthq. Eng.* **2021**, *140*, 106440. [[CrossRef](#)]
40. Kuznetsov, S.V. Seismic waves and seismic barriers. *Acoust. Phys.* **2011**, *57*, 420–426. [[CrossRef](#)]
41. Sun, Q.; Diasm, D.; Sousa, L. Soft soil layer-tunnel interaction under seismic loading. *Tunn. Undergr. Space Technol.* **2020**, *98*, 103329. [[CrossRef](#)]
42. Huang, Z.H.; Zhang, D.M. Scalar- and vector-valued vulnerability analysis of shallow circular tunnel in soft soil. *Transp. Geotech.* **2021**, *27*, 100505. [[CrossRef](#)]
43. Mh, A.; Aa, B. Performance-based analysis of tunnels under seismic events with nonlinear features of soil mass and lining. *Soil Dyn. Earthq. Eng.* **2021**, *134*, 106158. [[CrossRef](#)]
44. Zhang, Z.; Chen, F.; Li, N.; Swoboda, G.; Liu, N. Influence of fault on the surrounding rock stability of a tunnel: Location and thickness. *Tunn. Undergr. Space Technol.* **2017**, *61*, 1–11. [[CrossRef](#)]
45. Rayhani, M.H.T.; El Naggar, M.H. Numerical modeling of seismic response of rigid foundation on soft soil. *Int. J. Geomech.* **2008**, *8*, 336–346. [[CrossRef](#)]
46. Bilotta, E.; De Sanctis, L.; Di Larora, R.; D’Onofrio, A.; Silvestri, F. Importance of seismic site response and soil-structure interaction in dynamic behaviour of a tall building. *Geotechnique* **2015**, *65*, 391–400. [[CrossRef](#)]

**Disclaimer/Publisher’s Note:** The statements, opinions and data contained in all publications are solely those of the individual author(s) and contributor(s) and not of MDPI and/or the editor(s). MDPI and/or the editor(s) disclaim responsibility for any injury to people or property resulting from any ideas, methods, instructions or products referred to in the content.